JOURNAL OF GEOPHYSICAL RESEARCH, VOL. 114, XXXXXX, doi:10.1029/2007JB005505, 2009

Contemporary stress orientations from borehole breakout analysis in the southernmost flat-slab boundary Andean retroarc (32°44′ and 33°40′S)

Cecilia G. Guzmán[1,2] and Ernesto O. Cristallini[1,2]

Received 16 November 2007; revised 20 October 2008; accepted 23 December 2008; published XX Month 2009.

[1] Horizontal stress directions have been determined in the southernmost flat-slab boundary Andean retroarc between 32°44′ and 33°40′S within Cuyo Basin, Argentina. These directions were obtained from the borehole breakout analysis of 42 wells using four-arm caliper data. The mean maximum horizontal stress (SHmax) direction for the whole region is 104.1° with a 95% confidence interval of 8.1°. The present-day stress field has an approximately preferred E–W trend maximum horizontal stress direction, consistent with the plate boundary forces (80°) and the topographic forces (near E–W). The calculated SHmax directions are near the expected values, but some local deviations were observed. The SHmax rotates from an E–W orientation in the south to a NW–SE orientation to the north of this sector of the Andean retroarc. A regional variation in the stress field can be observed when these results for the Cuyo Basin are analyzed together with those presented in a previous study in the Neuquén Basin to the south. The maximum horizontal stress varies from ~NW–NE along this combined section of the Andean retroarc, with the ~E–W SHmax directions in the northern Neuquén Basin consistent with those observed in the southern sector of Cuyo Basin. These variations in the stress field orientation appear related with the topography geometry. From the analysis between the mean SHmax obtained and the acting forces, it can be concluded that the topographic control on the horizontal stress field seems to be dominant in the Cuyo Basin and in the north of Neuquén Basin. To the south of Neuquén Basin the horizontal stress field should be mainly controlled by the plate boundary forces.

Citation: Guzmán, C. G., and E. O. Cristallini (2009), Contemporary stress orientations from borehole breakout analysis in the southernmost flat-slab boundary Andean retroarc (32°44′ and 33°40′S), *J. Geophys. Res.*, *114*, XXXXXX, doi:10.1029/2007JB005505.

1. Introduction

[2] Much of the South American plate is now in horizontal compression and undergoing shortening, particularly along its western margin as shown by stress data compilations [*Assumpçao*, 1992; *Lima et al.*, 1997] and space-based geodetic results [*Kendrick et al.*, 2006]. It has long been recognized that great mountain belts are for the most part mainly built by contractional processes, and it is clear that during the last 10 My the contractional belts along the eastern margin of the Andes have accommodated most of the shortening that has occurred between the Pacific coast and the stable interior of the South American plate [*Kendrick et al.*, 2006]. Localized shortening in the Andean foreland continues in the present as evidenced by the concentration of shallow crustal seismicity [*Smalley and Isacks*, 1990; *Kendrick et al.*, 2006]. Tectonic stress data are fundamental for understanding the dynamics of mountain building, particularly when combined with topography, gravity or heat flow. The identification of regional stress distribution provides new insight into active tectonics, sedimentary basins evolution and earthquake potential [*Zoback*, 1992; *Tingay et al.*, 2005].

[3] Existing horizontal stress orientation data for South America is primarily determined from earthquake focal mechanisms, geological field observations of recent and active faulting and also from borehole breakouts and volcanic alignments information [*Assumpçao*, 1992; *Zoback*, 1992; *Colmenares and Zoback*, 2003; *Reinecker et al.*, 2005]. Recently, *Guzmán et al.* [2007] published a large number of horizontal stress data calculated from borehole breakout information from Neuquén Basin, in the Andean foreland of Argentina.

[4] This research is the continuation to the north of that previous work of *Guzmán et al.* [2007]. The new data were assembled throughout the southernmost flat-slab boundary in the Andean retroarc between 32°44′ and 33°40′S within Cuyo Basin; a hydrocarbon rich basin placed just 45–50 km to the north of the Neuquén Basin. Unlike the Neuquén Basin to

[1]Laboratorio de Modelado Geológico, Departamento de Ciencias Geológicas, Universidad de Buenos Aires, Buenos Aires, Argentina.
[2]Consejo Nacional de Investigaciones Científicas y Técnicas, Buenos Aires, Argentina.

0148-0227/09/2007JB005505$09.00

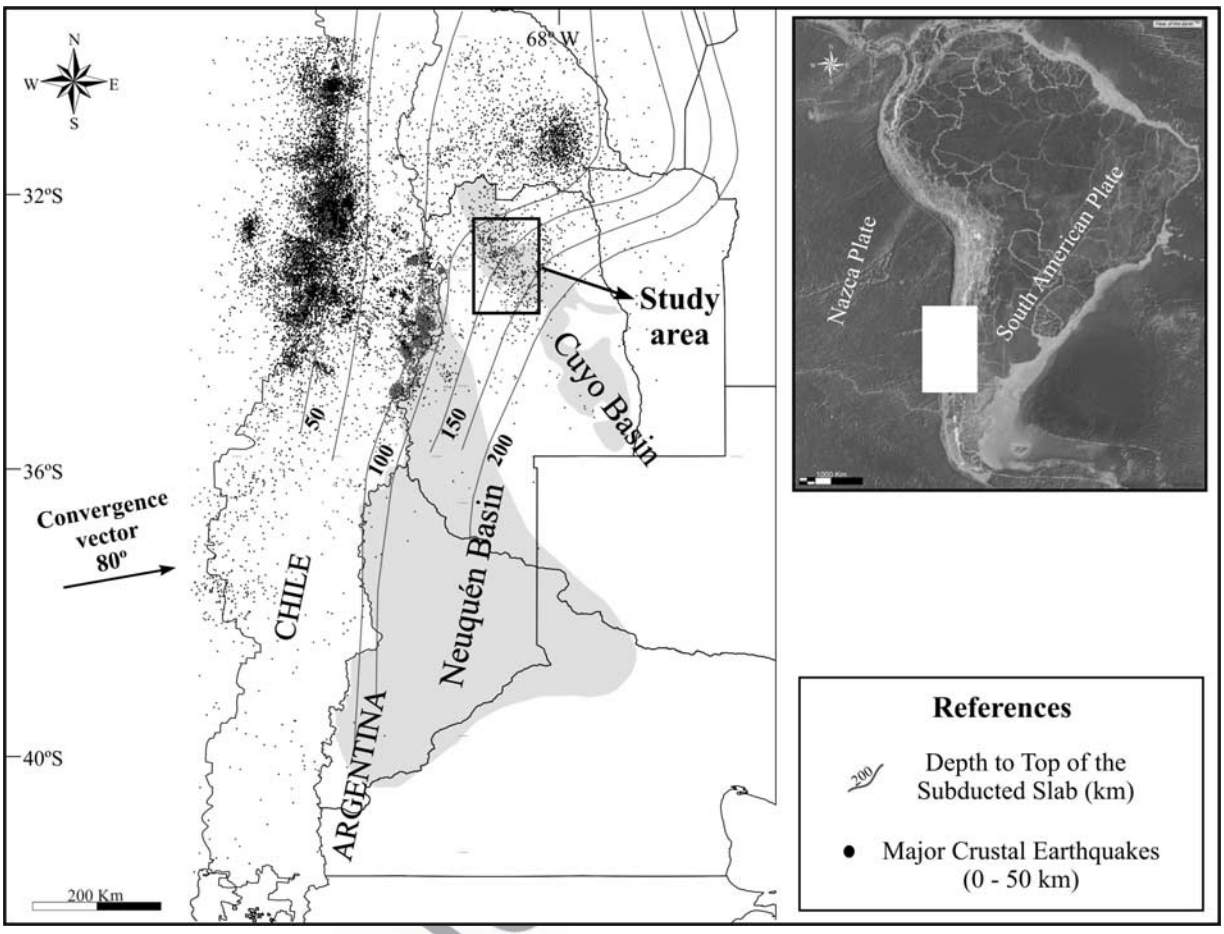

Figure 1. Major crustal earthquakes (from 0 to 50 km depth) [*National Earthquake Information Center* (*NEIC*), 2008]; the contour lines represent the depth to the top of the subducted slab in km [*Cahill and Isacks*, 1992]. Here it can be observed that for the Cuyo Basin area the subduction changes from flat subduction to a 30° dipping subduction zone. The study area is located in Argentina, South America, close to the Chilean border.

the south, this sector of the Andean retroarc has an important seismic activity; therefore, knowing the contemporary horizontal stresses is relevant not only in scientific terms and oil industry interest, but also can be potentially important for the study of seismic hazard (Figure 1). The study area includes the city of Mendoza which has almost 1,500,000 inhabitants and lies in the most seismically hazardous portion of Argentina [*Kadinsky-Cade et al.*, 1985; *INPRES*, 1982, 1995]. The city of Mendoza was completely destroyed by an earthquake (magnitude ~7) in 1861 and in 1985 was damaged by a ~6 magnitude earthquake with an epicenter ~35 km south from Mendoza city).

[5] Recent structural and active tectonics studies have contributed to understand the contemporary stress in the region. *Cortés et al.* [1999] studied the regional Quaternary tectonic in Mendoza province and later *Cortés et al.* [2000, 2005] made an analysis of the geometric patterns of Quaternary structures between 30°30′–33°30′S. *García* [2004], *García et al.* [2004], *Borgnia* [2004] and *Casa* [2005] analyzed the Neotectonic structure to the SW and W of Mendoza city. To the north of Mendoza province there are some focal mechanisms calculated and compiled by *Alvarado et al.* [2005]. They studied the earthquakes in the Andes between 29° and 36°S and determined that near Mendoza city the mean P and T axes azimuths are 82° and 156° with a plunge of 11° and 55° respectively. *Siame et al.* [2006] described the active tectonics in the Precordillera and western Sierras Pampeanas using focal mechanisms and faults kinematics. These authors increased the stress information; however, the in-situ stress data are still scarce.

[6] There are two SHmax orientations included in the World Stress Map database in the study area determined from earthquake focal mechanisms. In this paper, 42 new maximum horizontal stress directions (SHmax) determined from borehole breakouts analysis are presented. These horizontal stress directions are compared to predicted stress orientations on the basis of the present convergence vector, the direction of the ridge push and the topographic forces. A regional analysis of the obtained results is presented and discussed. The quality and the number of data presented in this work together with the results presented for the Neuquén Basin [*Guzmán et al.*, 2007] provide stress coverage for more than 800 km along strike in the Andean retroarc.

2. Tectonic Setting

[7] The data for this paper are obtained from wells drilled in the northwestern sector of Cuyo Basin, located in the

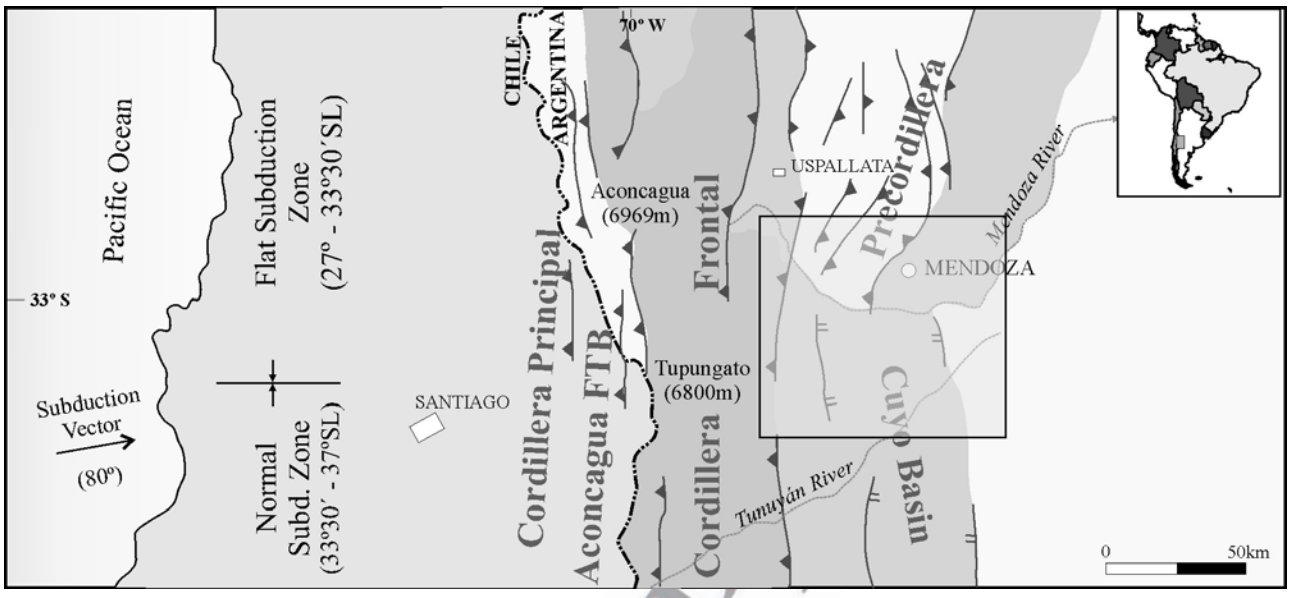

Figure 2. Major tectonic units of the Cuyo Basin (based on *Ramos et al.*'s [1996] information).

Central Andes foreland, between 32°44′ and 33°40′S in northwestern Mendoza Province of Argentina (Figure 1). The Cuyo Basin is one of the first discovered oil basins in Argentina and is part of a Triassic rift system partially inverted during the Cenozoic [*Uliana and Biddle*, 1988; *Legarreta et al.*, 1992; *Uliana et al.*, 1995]. The basin has a NW trend, oblique to the Andean structures.

[8] The Andean structure surrounding the study region is formed by different tectonic units (Figure 2); from W to E: the Aconcagua fold and thrust belt, the Cordillera Frontal and the Precordillera [*Kozlowski et al.*, 1993]. This Andean structure is partially overimposed to the Cuyo Basin. The Aconcagua fold and thrust belt [*Ramos*, 1988; *Mpodozis and Ramos*, 1989] is characterized by a number of thin-skinned imbricate thrusts [*Ramos*, 1985], mainly involving post Jurassic units. The Cordillera Frontal is thick-skinned and is characterized by large pre-Jurassic basement blocks uplift. The Precordillera, at this latitude, is divided into two sectors with different structural behavior [*Kozlowski et al.*, 1993]. The central Precordillera, dominated by high-angle thrusts and strike slip accommodation faults, and the western Precordillera characterized by an eastern vergence [*Kozlowski et al.*, 1993].

[9] At the present, the western margin of this part of South America is characterized by the subduction of the Nazca Plate beneath the continental South American Plate with an 80° convergence vector [*Angermann et al.*, 1999; *Norabuena et al.*, 1999; *Kendrick et al.*, 2003]. It is segmented into a flat subduction zone north of 33°S and a 30° dipping subduction zone to the south [*Isacks et al.*, 1982; *Jordan et al.*, 1983; *Sarewitz*, 1988]. The study area is within the boundary between these two subduction segments [*Bevis and Isacks*, 1984] (Figure 1). In this Andean region, the flat slab geometry is attributed to the subduction of the Juan Fernandez Ridge below the South American margin [*Pilger*, 1981], and expressed at the magmatic arc by a change in the geochemistry properties of the Neogene volcanism and a cessation of activity at roughly 10 Ma [*Kay and Abbruzzi*, 1996; *Siame et al.*, 2005]. As suggested by *Gutscher et al.* [2000], flat subduction could alter the thermal structure of the margin, cooling both, upper and subducting plates, and thus greatly increases the strength of the upper lithosphere.

[10] The Quaternary deformation along the southern edge of this flat subduction zone has mainly been recognized in the eastern and western margins of the Precordillera [*Cortés et al.*, 2000; *Borgnia*, 2004; *Casa*, 2005] where Paleozoic to Quaternary strata are involved in the Andean deformation (<20 Myr) [*Siame et al.*, 2005]. The information processed in this paper is just to the east of the Precordillera, where the active tectonic front of the Andes is advancing over the foreland. The southernmost boundary of the Precordillera is related to the transition between flat-slab subduction and the 30° dipping subduction zone.

[11] The Quaternary faults of the region are located to the east of the Cordón del Plata, represented by blind thrusts dipping to the west. Some evidences for the presence of these thrusts are changes in the relief in the foot-hill zone, folding of some fluvial terraces, and several fault scarps [*Cortés et al.*, 1999; *García*, 2004; *García et al.*, 2004; *Vergés et al.*, 2007].

[12] *Miranda and Robles* [2002] studied the Bouguer's anomaly in Cuyo Basin and they saw that the isostatic anomalies are positive indicating that it is in a slight overcompensation. This indicates the possibility of potential vertical descending movements. Consequently, in the future, Cuyo Basin should subside to reach the equilibrium.

2.1. Stress Field Models

[13] *Coblentz and Richardson* [1996] made three different stress models for South American Plate; they concluded that the stress field results from the interaction of two principal tectonic processes, the buoyancy or topographic forces and compressional stresses transmitted across plate boundaries. They proposed that the origin of the E–W compressive stress regime is the result of the interaction between the ridge push force and the collisional forces acting along the western margin of the continent. The approach of *Meijer et al.* [1997] is an improvement of previous work on the Andes [e.g.,

Dalmayarc and Molnar, 1981; *Richardson and Coblentz*, 1994] in which the state of the stress in the mountain range has been addressed only in terms of vertical cross section. Their models also have some differences with the *Coblentz and Richardson*'s [1996] model, especially because different types of forces are included. *Meijer et al.* [1997] concluded that a uniform distribution of the resistance on the western margin of South America provides a better overall fit to the available observations than a dip-dependent distribution of resistance magnitude. Their results also suggest that an extra driving force, additional to ridge push, may be acting on the South American Plate to ''sustain'' the Andean Cordillera.

2.2. Velocity Field Models

[14] *Brooks et al.* [2003] studied the velocity vector field for the Andes Mountains between 26° and 36°S. They propose the presence of an Andean ''microplate'' modeled between the Nazca and South American plates (Figure 3). The Andean ''microplate'' boundary corresponds with the geologically youngest structures of the thrust front. Their model is based not only on GPS measured velocity vectors but also on the abundant seismic activity concentrated on the front of the Andean ''microplate''. In their analysis they test the hypothesis that the orogen itself behaves as a rigid unit. They observed that adding the Andean microplate to the traditional description of Nazca-South American plate convergence provides the kinematic framework for nearly complete explanation of the observed velocity field. Notably, the velocity field shows no obvious or abrupt change in character associated with the changing dip of the subducted Nazca plate. Additionally, in their model, permanent deformation is not accumulating throughout the backarc contractional wedge; the deformation is developed only within a narrow deformational zone on the backarc.

3. Borehole Breakout Identification Technique

[15] One of the oldest techniques for borehole breakout identification is using four-arm caliper data included in routine dipmeter logs. In the last years, more sophisticated and precise methods for breakout identification have been developed using borehole images (i.e., Ultrasonic Borehole Imager, Fullbore Formation Micro Imager Log, Full Bore Scanner Tool). However, the standard dipmeter logs are particularly useful in basins where the exploration period was concentrated before new techniques were available.

[16] Four-arm caliper dipmeter logs were used in this study. The caliper tool rotates as it ascends during logging registration because of cable torque. Well diameter and reference arm orientation are continuously measured. When an elongation is present in the well bore, the caliper pairs are differentially extended, the tool stops rotation and a constant direction is recorded for the reference arm [*Zerwer and Yassir*, 1994]. In this study the breakouts were human detected following the criteria suggested by the World Stress Map [*Reinecker et al.*, 2004].

[17] 1. Tool rotation must cease in the zone of enlargement.

[18] 2. There must be clear tool rotation into and out of the enlargement zone.

[19] 3. The smaller caliper reading is close to bit size. Top and bottom of the breakout should be well marked.

[20] 4. Caliper difference has to exceed bit size by 10%.

[21] 5. The enlargement orientation should not coincide with the high side of the borehole in wells deviated by more than 5°.

[22] 6. The length of enlargement zone must be greater than 1 m.

[23] The combined use of these six criteria enables to detect and distinguish zones of breakouts from other borehole distortions such as washouts and key seats [*Reinecker et al.*, 2004]. In this research only vertical wells (deviation <5°) have been used to avoid key seat misidentification instead of breakout.

[24] In order to determine mean breakout orientations circular statistics has to be used. Taking into account that breakout orientations are bimodal data; data between 180° and 360° are equivalent to those between 0° and 180° [*Reinecker et al.*, 2004]. As said by *Mardia* [1972] the mean breakout azimuth (θ_m) of a population of n picked breakout directions θ_i is derived by first transforming the angles to the 0–360° interval.

$$\theta_i^* = 2\theta_i$$

[25] The direction cosine and sine have to be added and averaged by the total length L (length weighted mean) [*Reinecker et al.*, 2004].

Length weighted

$$L = \sum_{i=1}^{n} l_i$$

$$C = \frac{1}{L}\sum_{i=1}^{n} l_i \cos\theta_i^*$$

$$S = \frac{1}{L}\sum_{i=1}^{n} l_i \sin\theta_i^*$$

where l_i is the length of breakout i with orientation θ_i^*.

[26] The mean azimuth results from $\theta_m = \frac{1}{2}\arctan(S/C)$.

[27] The angular standard deviation is ($D(\theta_m)$) derived as

$$D(\theta_m) = \frac{1}{n}\sum(\pi - |\pi - |\theta_i - \theta_m||)$$

[28] The data have been ranked according to the World Stress Map quality ranking scheme [*Zoback and Zoback*, 1989, 1991; *Sperner et al.*, 2003]. The classification allows the comparison of different indicators of tectonic stress (e.g., focal mechanism solution, drilling-induced tensile fractures, overcoring, etc. [*Reinecker et al.*, 2004]). The ranking scheme is based mainly on the number, accuracy, and length of measurements and is given in Table 1.

4. Results

[29] Only a fraction of wells drilled within the Cuyo Basin were available for this study and had the information needed to calculate the breakout orientation. The well information was provided by REPSOL-YPF oil company. From the company database about 100 wells distributed throughout

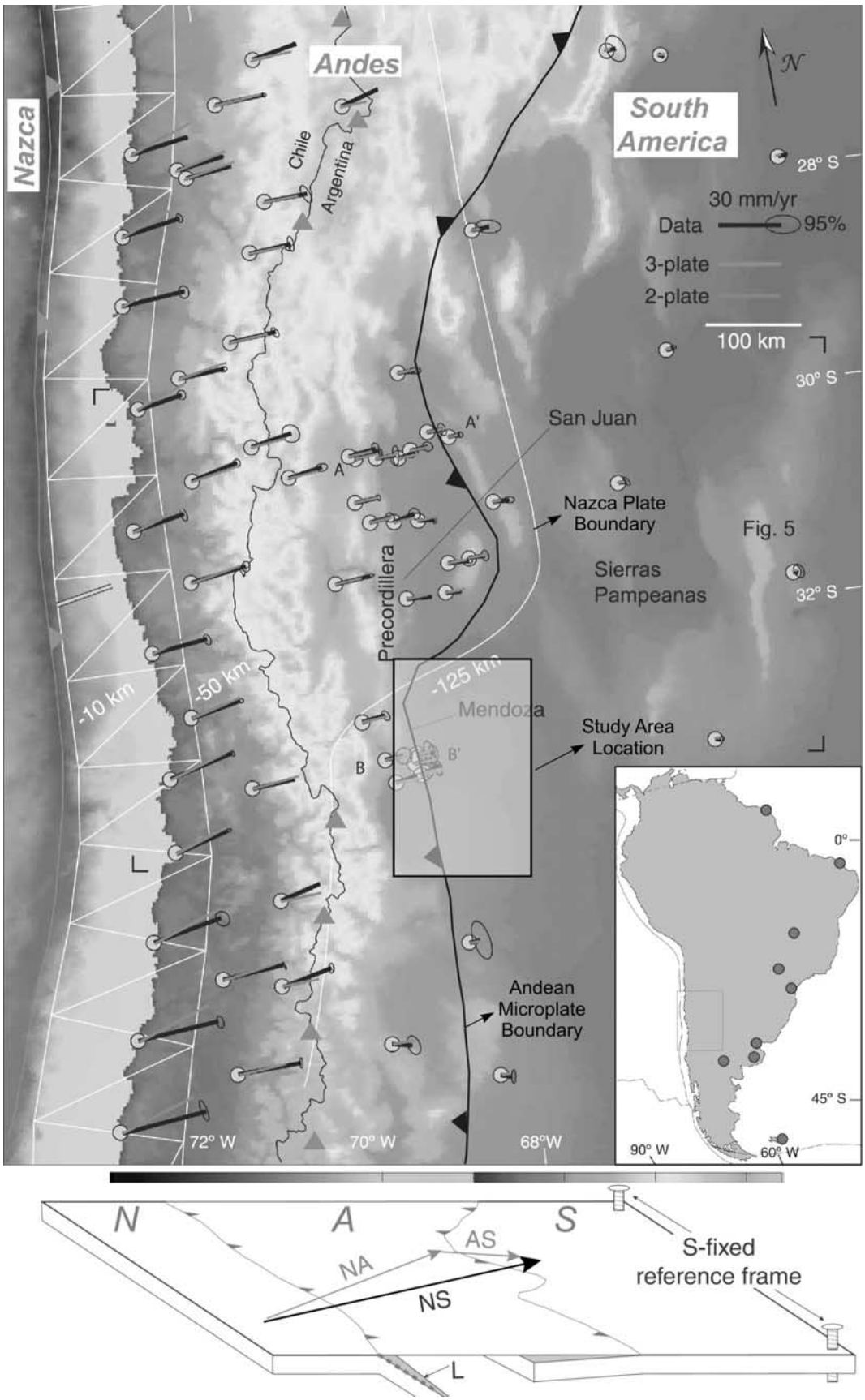

Figure 3. Velocity stress field calculated by *Brooks et al.* [2003] overimposed to the Andean topography. The map indicates the Andean ''microplate'' boundary modeled by these authors between the Nazca and South American plates and it also delimits the study area's location.

t1.1 **Table 1.** Quality Criterions Used by the World Stress Map Project [*Sperner et al.*, 2003]

t1.2	A	B	C	D	E
t1.3	Wells that have ten or more distinct breakouts zones with a combined length >300 m and with a standard deviation $\leq 12°$	Wells that have at least six distinct breakout zones with a combined length >100 m and with a standard deviation $\leq 20°$	Wells that have at least four distinct breakout zones with a combined length >30 m and with a standard deviation $\leq 25°$	Wells that have less than four breakout zones or a combined length <30 m or with a standard deviation >25°	Wells with no reliable breakouts detected or with extreme scatter of breakout orientations (standard deviation >40°)

the northwest sector of the Cuyo Basin were obtained; 50 of them had the required information and were utilized to determine the breakout. The others only have partial information and no breakout information could be obtained. From the 50 selected data, 42 of them yielded a mean breakout direction. In the eight wells that did not yield breakout data, caliper 1 was very similar to caliper 2, hence there was essentially no elongation. The lack of elongation and breakouts could either indicate nearly equal horizontal stress or high rock strength.

[30] For each well breakout segments were identified from four-arm caliper data. The mean breakout orientation and the standard deviation for the entire well were calculated. The data were ranked using World Stress Map Project criterions (Table 1). Breakout orientations are perpendicular to the maximum horizontal stress (SHmax) directions; therefore SHmax directions can be easily calculated. Table 2 lists the 42 wells with their location, the mean SHmax direction with its respective standard devi0ations (weighted by length), the number of intervals interpreted for each well, the accumulated length, the quality ranking and the depth interval where breakouts were recognized. It is important to take into account that the depth of the breakout interval analyzed will depend on the depth where the company sampled the well.

[31] The SHmax orientation interpreted for the 42 wells analyzed is illustrated in Figure 4. The stress data are well

t2.1 **Table 2.** List of the 42 Wells Analyzed Within the Mendoza Retroarc[a]

t2.2	Well	Lat.	Long.	Mean SHmax Direction Weighted by Length	Standard Deviation	Breakout Intervals	Accumulated Length	Quality	Depth Range (m)
t2.3	1	−33.64	−68.54	83	18.0	7	127.3	B	1247.25–1697.75
t2.4	2	−33.55	−68.67	93	14.1	11	272.3	B	1779–2132.5
t2.5	3	−33.40	−68.50	102	10.8	3	38.8	D	2273.5–2414.5
t2.6	4	−33.37	−69.05	98	5.2	6	160.8	B	3333–3908.25
t2.7	5	−33.36	−69.06	102	17.8	10	330.2	B	3288.25–3797.94
t2.8	6	−33.35	−69.06	99	0.1	2	263.1	D	3156–3429
t2.9	7	−33.34	−68.56	85	7.1	19	313.0	A	2481–3472.75
t2.10	8	−33.34	−68.68	96	8.7	20	785.5	A	971–3245.5
t2.11	9	−33.31	−68.96	112	5.0	9	292.3	B	413–3399.75
t2.12	10	−33.31	−68.98	111	8.3	9	510.8	B	2914.75–3494.66
t2.13	11	−33.31	−68.96	113	1.5	1	13.8	D	3135.25–3149
t2.14	12	−33.29	−68.93	120	4.3	16	182.3	B	3124.5–3604
t2.15	13	−33.28	−68.85	105	10.9	11	377.3	A	2831–3337.5
t2.16	14	−33.28	−68.85	108	3.1	7	501.5	B	2735.5–3309.75
t2.17	15	−33.27	−68.73	108	10.7	9	267.8	B	2377.5–2917.5
t2.18	16	−33.25	−68.72	94	17.3	4	44.5	C	2751.25–2828
t2.19	17	−33.25	−68.80	112	3.9	4	258.8	C	2534–2805
t2.20	18	−33.24	−69.00	118	12.1	10	204.3	B	3153.25–3869.5
t2.21	19	−33.24	−68.75	115	3.5	10	583.4	A	2071.93–2848.89
t2.22	20	−33.21	−68.79	20	56.0	5	307.2	E	2741.25–3179.44
t2.23	21	−33.19	−68.76	106	8.2	6	726.0	B	1125.46–2388.76
t2.24	22	−33.19	−68.76	119	25.4	12	167.3	D	2155.25–2645.5
t2.25	23	−33.19	−69.07	112	48.5	14	925.2	E	2000.41–3802.29
t2.26	24	−33.17	−69.09	98	21.0	7	632.8	C	1862–3331.53
t2.27	25	−33.16	−69.02	92	5.1	16	264.3	B	3612.25–4058.25
t2.28	26	−33.15	−68.79	105	2.2	1	31.0	D	2336.75–2367.75
t2.29	27	−33.15	−68.77	4	26.0	2	22.3	D	492.5–656.75
t2.30	28	−33.15	−68.78	116	15.5	21	229.8	B	320–2530.75
t2.31	29	−33.15	−68.84	94	8.1	4	124.5	C	3202.5–3501.5
t2.32	30	−33.14	−68.75	103	17.0	23	1957.4	B	1200.5–3810.22
t2.33	31	−33.14	−69.17	74	28.6	6	95.8	D	3301.75–3509.25
t2.34	32	−33.13	−69.08	106	17.1	20	714.2	B	2861–3644.91
t2.35	33	−33.13	−68.78	125	10.2	8	320.4	B	2067.61–2586.25
t2.36	34	−33.13	−68.77	82	17.5	11	292.0	B	1884–2370
t2.37	35	−33.12	−68.78	124	7.1	4	56.8	C	2379.25–2453.25
t2.38	36	−33.12	−68.78	98	17.6	13	639.7	B	1893.92–2797.54
t2.39	37	−33.11	−68.80	101	1.7	4	342.8	C	1963.25–2420
t2.40	38	−33.11	−68.78	109	24.2	12	279.5	C	2158.25–2689
t2.41	39	−33.11	−69.09	124	29.6	26	2030.9	D	600.12–3216.87
t2.42	40	−33.08	−68.99	94	24.1	9	601.0	C	3301–4161.14
t2.43	41	−33.04	−69.21	128	28.8	18	774.4	D	504.25–1884
t2.44	42	−32.74	−68.84	119	18.0	6	137.5	B	3472.25–3708

t2.45 [a]For each well, the mean SHmax orientation weighted by length and by number of breakout intervals, the standard deviation for the whole well, the quality using World Stress Map Project criterions (see Table 1), and the depth range are shown.

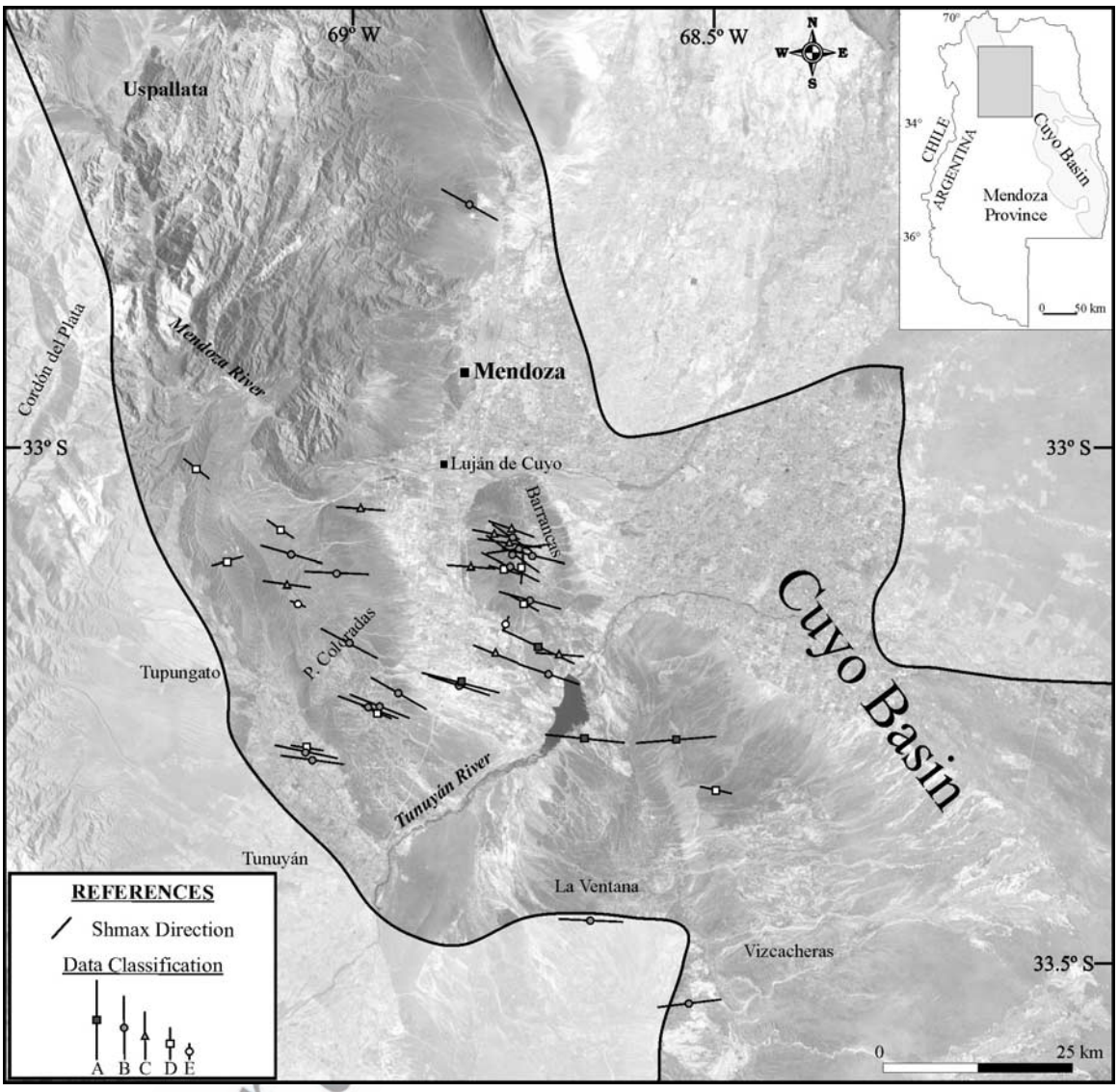

Figure 4. Orientation and classification of maximum horizontal stress from 42 bore wells within the Cuyo Basin. The different symbol size corresponds to SHmax ranking quality using the World Stress Map criteria. The Cuyo Basin boundary is shown with a solid line.

distributed within the basin and give a coherent picture of SHmax orientation (Table 2 and Figure 4). The data were recorded between depths of 320 and 4161.15 meters. Most of the SHmax orientations have a relative low to medium dispersion about the well mean orientation. Using World Stress Map Project criterions (Table 1), 4 data were ranked as A, 19 as B, 8 as C, 9 as D and 2 as E (see Table 2). More than the 74% of the data have a standard deviation smaller than 25°, 22% have a standard deviation between 25° and 40° and only the 4% are not useful.

[32] The horizontal stress direction can change in a well when a fault or an important detachment level is crossed. The study area is structurally active and one of these situations could be possible. In order to identify any regional near-horizontal detachment or fault system, there relation between depth and breakout orientation was analyzed. No relation could be established between breakout orientation and depth in the analyzed region (Figure 5; a complete analysis can be found in the work of *Guzmán* [2007]).

[33] The SHmax orientations have been plotted in two rose diagrams (Figure 6). In the first one (Figure 6a) A–D quality data were used and in the second (Figure 6b) only A–C quality data were computed. The distribution for the first diagram has a preferred trend with a resultant direction of azimuth 105.4° and a 95% confidence interval of 9.6°. The second one has a resultant direction of azimuth 104.1° and a 95% confidence interval of 8.1°. In spite of the fact that there are no significant differences between both mean directions, the D data are generally considered unreliable because of their great dispersion or because only short intervals were sampled, therefore only the data from A to C were used in the following analysis.

[34] In a general view, SHmax is oriented near WNW–ESE direction; however it is not completely uniform within the whole area. In Figure 4 it can be recognized some SHmax directions which do not follow the general trend. The SHmax orientation changes slightly through the study area: to the north it has a NW–SE direction is supported by a few data,

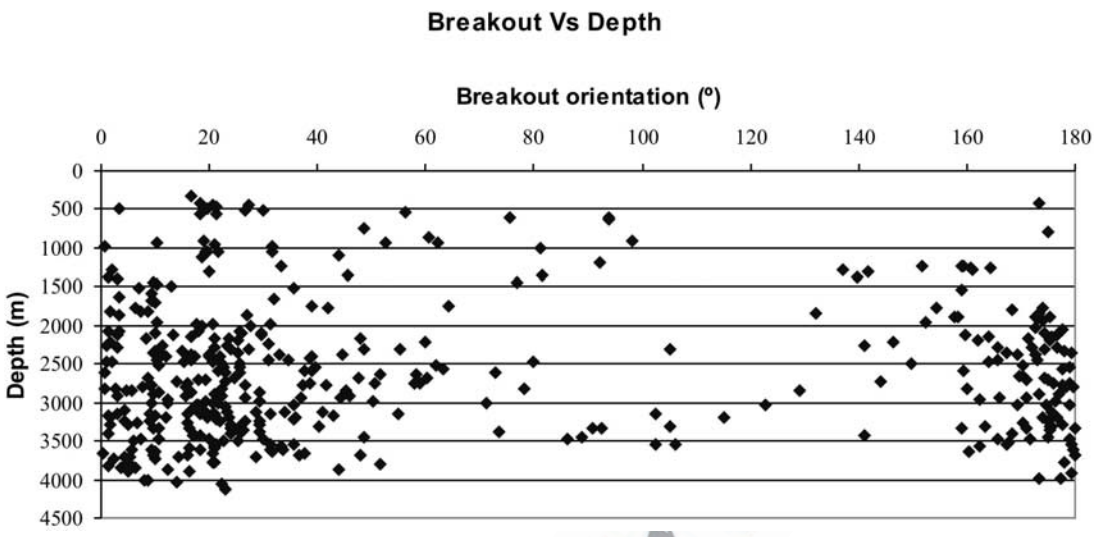

Figure 5. Borehole breakout interval orientations achieved for each well analyzed versus depth. It can be seen that there is no direct relation between breakout direction and depth.

and to the south an E–W to WNW–ESE orientation is well documented, close to the directions obtained for the northern Neuquén Basin [*Guzmán et al.*, 2007].

[35] The SHmax directions calculated in this paper were compared with the existing stress data for this region from other sources. Figure 7 shows the SHmax directions calculated from borehole breakouts (this paper) with the maximum horizontal stress data obtained from the World Stress Map Project calculated from focal mechanisms [*Reinecker et al.*, 2005]. It can be seen that all the data are consistent along the analyzed region, reinforcing the data consistency.

5. Interpretation and Discussion

[36] To analyze the horizontal stress field it is necessary to know and understand the forces acting on the study area. For this sector of the Andean retroarc, the SHmax orientation may be controlled by both, the convergence vector between the

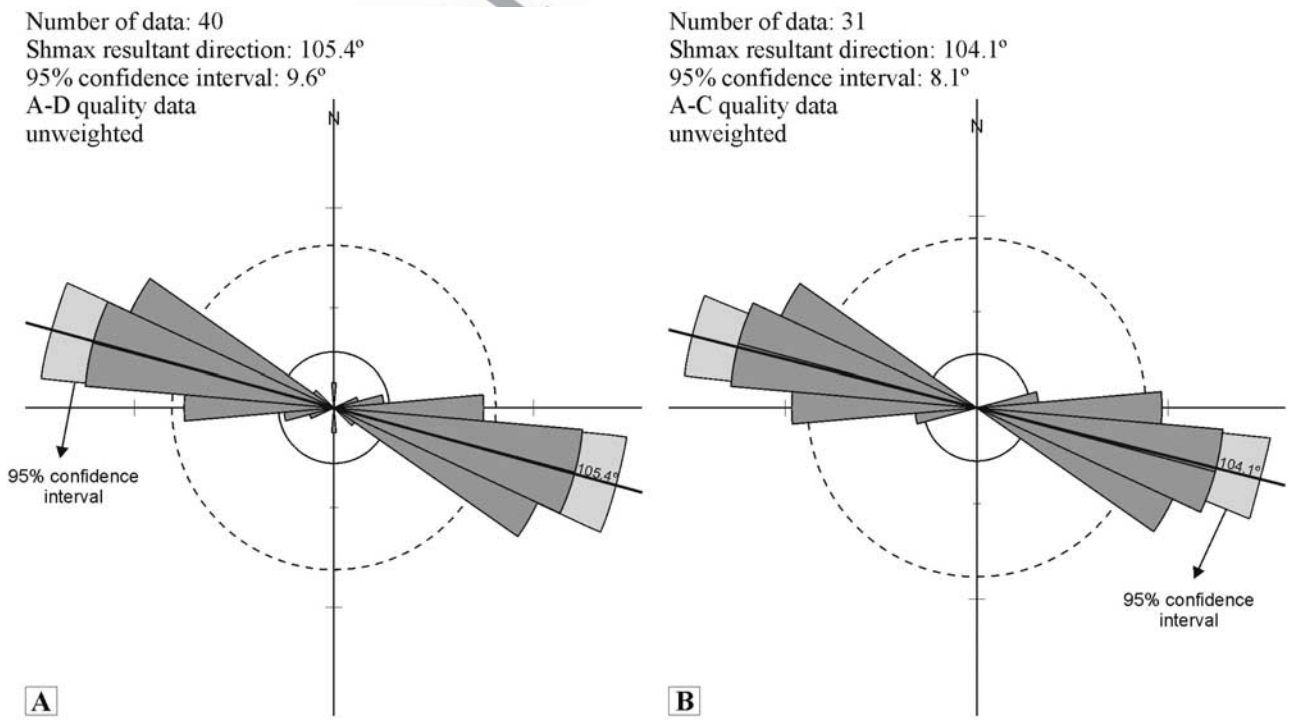

Figure 6. Rose diagram for the SHmax orientations. (a) Rose diagram of all the data with qualities ranking from A to D. The distribution has a preference trend with a resultant direction of azimuth 105.4° and a 95% confidence interval of 9.6°. (b) Rose diagram of all the data with qualities ranking from A to C. The distribution has a preference trend with a resultant direction of azimuth 104.1° and a 95% confidence interval of 8.1°.

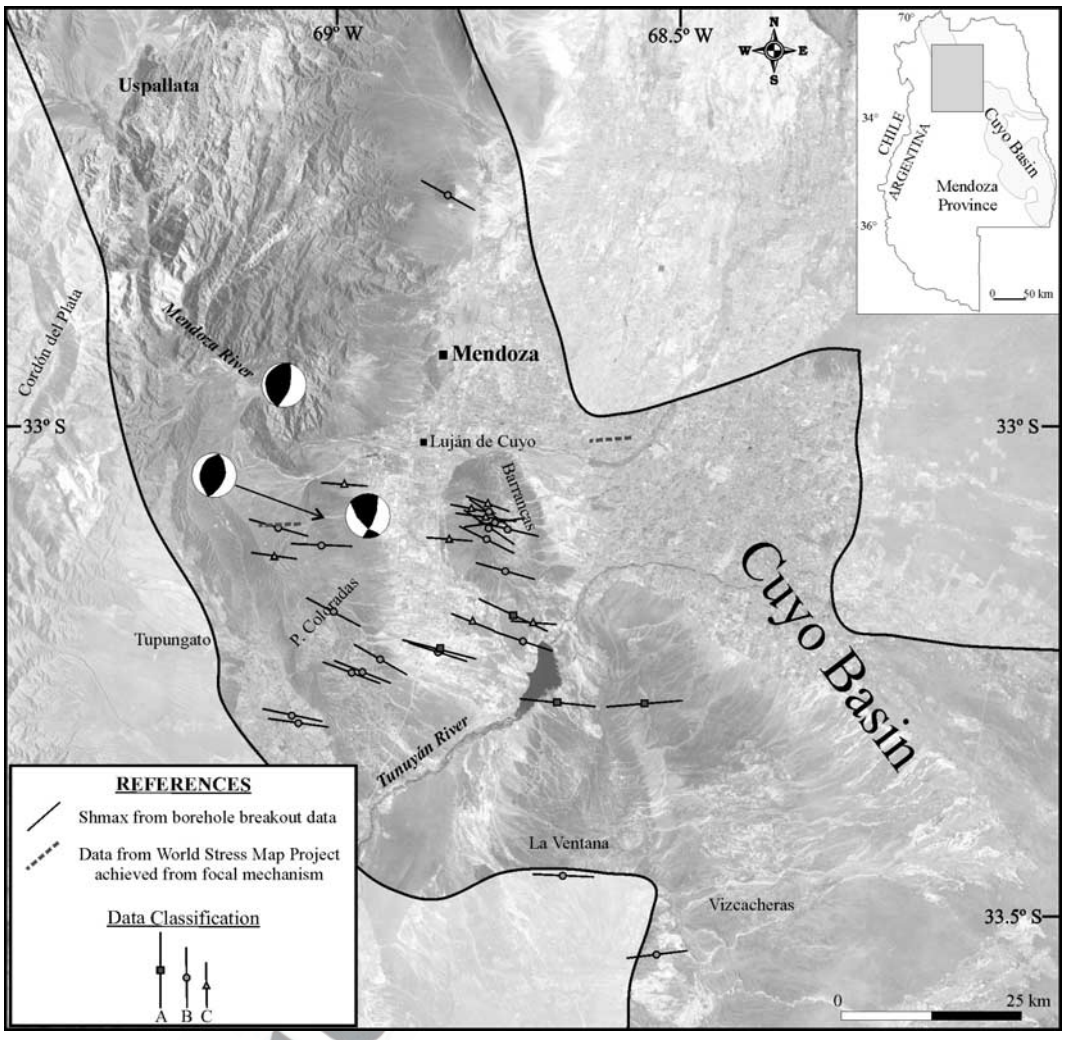

Figure 7. SHmax directions (A–C) calculated from borehole breakouts compared with the SHmax data achieved from the World Stress Map Project from focal mechanisms [*Reinecker et al.*, 2005]. The focal mechanisms calculated by *Alvarado et al.* [2005] are also shown; it can be observed that, taking into account these focal mechanisms, the stress regimen for this sector of the Andean retroarc is compressive.

Nazca and South American plates (azimuth 080°) [*Angermann et al.*, 1999; *Norabuena et al.*, 1999; *Kendrick et al.*, 2003; *Guzmán et al.*, 2007], the direction of the ridge push (E–W) and the topographic forces (in general E–W, just perpendicular to the main topography axis). All of these forces are acting approximately with an E–W orientation in this segment of the South American Plate [*Coblentz and Richardson*, 1996; *Meijer et al.*, 1997]; consequently, the expected SHmax orientation should be approximately parallel to them. The compressive stress regimen in this area is well documented by the focal mechanisms calculated by *Alvarado et al.* [2005] (see Figure 7) and the SHmax orientations obtained in this work are near the expected values (see Table 2 and Figure 6). However, some local anomalies are lightly recognized in the SHmax orientation within the study zone (Figures 6 and 7) and more strongly recognized comparing with Neuquén Basin data.

[37] To the south of Cuyo Basin, the SHmax fluctuates between W–E and WNW–ESE orientation, and to the north it is around NW–SE, near perpendicular to the general structural trending. This north to south variation is coinciding with the southern end of the Precordillera and the NW–SE northernmost data of this work are near perpendicular to the NE trending of this tectonic unit. However, only a few data support this northern change in SHmax direction (see Figures 2, 4, and 7).

[38] Nevertheless, when the full extent of stress data available for the Cuyo and Neuquén Basins are analyzed together a regional variation in stress field orientation from south to north is more clearly revealed (Figure 8). The obtained SHmax for the whole Neuquén Basin has a preferred trend with a resultant direction of azimuth 88.7° and a 95% confidence interval of 13.3° [*Guzmán et al.*, 2007]. However, the horizontal stress trajectory map achieved for this basin shows that the SHmax is not completely uniform. Within Neuquén Basin a NE direction was found, probably showing a basement structural control in the stress field geometry [*Guzmán et al.*, 2007]. When the whole region (both basins) is analyzed, is clear to see that to the south of Neuquén Basin, the mean SHmax orientation is WSW–ENE [*Guzmán et al.*, 2007], to the north of Neuquén Basin and south of Cuyo Basin, the SHmax direction fluctuates between W–E and

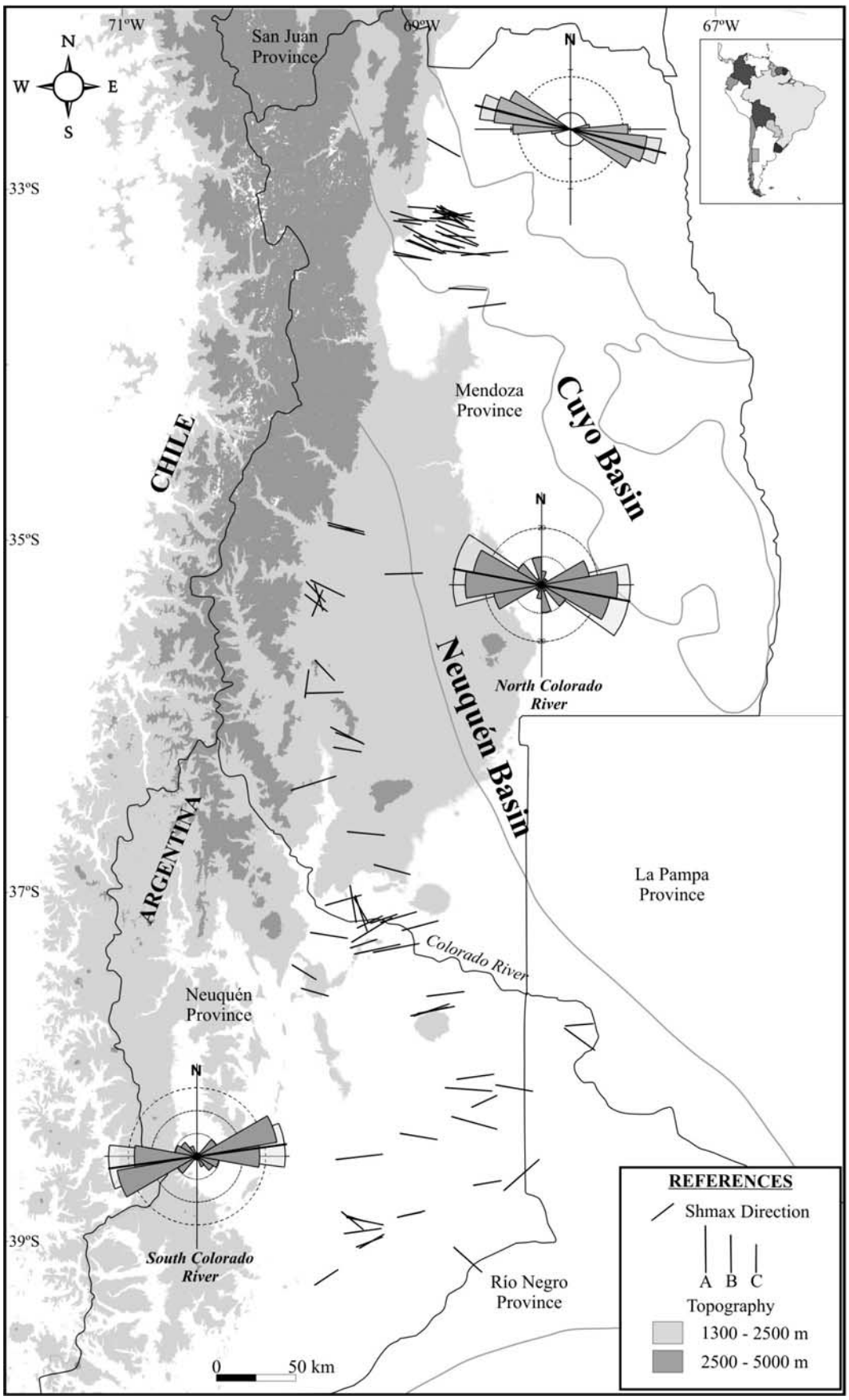
71°W
69°W
67°W
N
W
E
S
San Juan Province
33°S
35°S
37°S
39°S
CHILE
ARGENTINA
Mendoza Province
Cuyo Basin
Neuquén Basin
North Colorado River
South Colorado River
Colorado River
Neuquén Province
La Pampa Province
Río Negro Province
0
50 km
REFERENCES
Shmax Direction
A B C
Topography
1300 - 2500 m
2500 - 5000 m

Figure 8

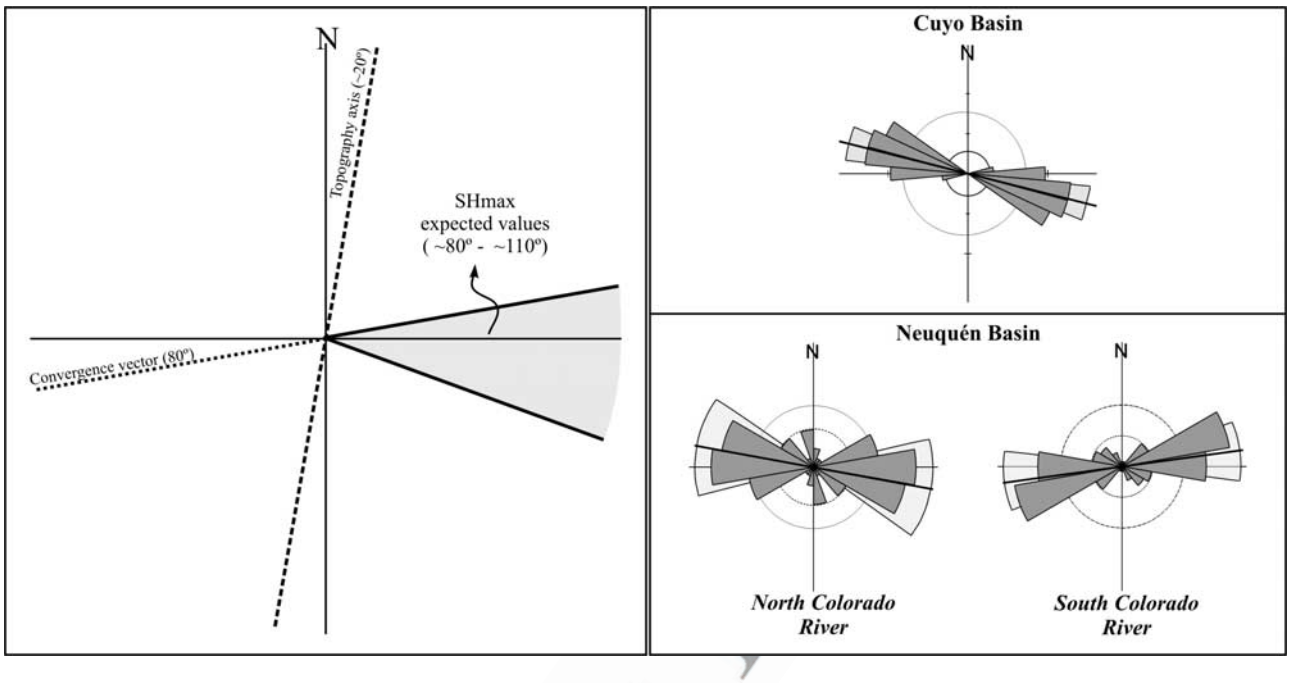

Figure 9. Main forces acting in this sector of the Andean retroarc, and the expected SHmax values. The close relationship between the topography orientation and the SHmax direction observed in the north sector of Neuquén Basin and in Cuyo Basin indicates that the stress field there is controlled by the topography. This relation to the south of Neuquén Basin is not so clear; this suggests that the stress field there is mainly controlled by the plate boundary forces.

WNW–ESE and to the northern Cuyo Basin sector it changes to a NW–SE direction. This last change is poorly supported because only a few data are available.

[39] When the relationship between the horizontal stress field and the topography axis is analyzed there seems to be a close connection. The SHmax direction is almost perpendicular to the topography. *Guzmán et al.* [2007] proposed two possible explanations for the stress field orientation in the Neuquén Basin, suggesting that either the topographic forces exert an important control on the stress field, or that ancient structural indenters (rigid block moving eastward) are controlling the horizontal stress field. The first hypothesis has been previously mentioned by other authors [*Coblentz and Richardson*, 1996; *Meijer et al.*, 1997] and the SHmax results obtained in this paper are coherent with them. In the Cuyo Basin the close connection between the SHmax orientation and the topography can be seen in Figure 7, where the SHmax is almost-perpendicular to the topographic axis.

[40] The second hypothesis relates the stress field to the presence of structural indenters, and is based on *Brooks et al.*'s [2003] proposal of an Andean "microplate" between the Nazca and South American plates. Their model is based not only on GPS measured velocity vectors but also on the abundant seismic activity concentrated on the front of the Andean "microplate". This activity is present near the topographic front in the Cuyo Basin (see Figure 1), but is absent in the Neuquén Basin.

[41] In Figure 9 the different forces acting in the Cuyo basin sector of the Andean retroarc are represented. The plate boundary forces (azimuth 80°) and the forces related with either buoyancy or the action of structural indenter (azimuth ~110°) are indicated. When the stress field is analyzed it can be observed that the SHmax direction obtained in this research (azimuth ~104°) is within the expected ones. However, this last value seems to have signature of both type of forces showed in Figure 9 since this direction cannot be only explained with the plate boundary force. When the Neuquén Basin results are analyzed it can be observed that there are two different sectors. To the north of the Colorado River, the SHmax mean orientation is similar to the mean SHmax calculated in Cuyo Basin, indicating that the topography here is also exerting an important control in the stress field. To the south of Colorado River this relation between the stress field and topography is less clear, here the mean SHmax is very close to the convergence vector indicating that the stress field for this sector is mainly controlled by the plate boundary forces. This seems to be reasonable because the elevations south of Colorado River are smaller than to the north were the higher topography is registered just to the west of Cuyo Basin area (Figure 8).

[42] The previous discussion is somewhat qualitative, with the data presented here and in the work of *Guzmán et al.* [2007] it is not possible to discern which of the different source of forces analyzed is exerting a higher control in the

Figure 8. SHmax from borehole breakout data for Cuyo and Neuquén Basins (A–C). It can be observed that there is a regional tendency in the stress field variation from south to north. The northern SHmax direction in the Neuquén Basin is consistent with the direction observed in the southern sector of the Cuyo Basin. There is a change in the SHmax orientation in the Neuquén and Mendoza retroarc along an N–S axis.

horizontal stress field and which model (indenter or topographic forces) has a better fit for each zone. A detailed comparison between the horizontal stress and local topographic features is the next step of this research. Numerical models are needed to understand the local variations in the stress field and their relation with topography.

6. Conclusions

[43] The horizontal stress field acting between 32°44′ and 33°40′S has been calculated from borehole breakout analysis of 42 wells drilled within the Cuyo Basin. A mean SHmax orientation of 104.1° with a 95% confidence interval of 8.1° was obtained for this portion of the Andean retroarc, using the data classified from A to C (World Stress Map classification). The data obtained in this paper and in the paper of *Guzmán et al.* [2007] represent a very important contribution to the stress field picture of South America.

[44] The SHmax directions are generally within the expected values, near the convergence subduction vector orientation (80°), but some variations in the stress field orientation appear related with the topography geometry. The close relationship between the SHmax orientation and the direction perpendicular to the topographic axis suggests that the stress field induced by the subduction forces is also controlled or modified by the topography.

[45] The northern SHmax direction in the Neuquén Basin is consistent with the direction observed in the southern sector of Cuyo Basin. When Cuyo and Neuquén Basins are analyzed together it can be observed that there is a regional tendency in the stress field variation from south to north. From the analysis between the mean SHmax obtained and the acting forces, it can be observed that the topographic control on the horizontal stress field is dominant in the Cuyo Basin where the maximum elevations are founded (more than 4500 m). To the south of Neuquén Basin, where the elevations are so much smaller (less than 2500 m), the horizontal stress field is mainly controlled by the plate boundary forces.

[46] **Acknowledgments.** We want to express our gratitude to REPSOL-YPF for providing the data needed for this research, especially to Silvia Zencich and Ricardo Calegari. This study has been done with funding from Agencia Nacional de Promoción Científica y Tecnológica PICT 38295, CONICET (PEI 6465/04 and PEI 5758/05) and Universidad de Buenos Aires (Proyecto UBACyT, Ernesto Cristallini).

References

Alvarado, P., S. Beck, G. Zandt, M. Araujo, and E. Triep (2005), Crustal deformation in the south-central Andes backarc terranes as viewed from regional broad-band seismic waveform modeling, *Geophys. J. Int.*, doi:10.1111/j.1365-246X.2005.02759.x.

Angermann, D., J. Klotz, and C. Reigber (1999), Space-geodetic estimation of the Nazca-South America Euler vector, *Earth Planet. Sci. Lett.*, *171*, 329–334.

Assumpçao, M. (1992), The regional intraplate stress field in South America, *J. Geophys. Res.*, *97*, 11,889–11,903.

Bevis, M., and B. Isacks (1984), Hypocentral trend surface analysis: Probing the geometry of Benioff zones, *J. Geophys. Res.*, *89*, 6153–6170.

Borgnia, M. (2004), Neotectónica del piedemonte oriental del cordón del Plata al norte del río Blanco, provincia de Mendoza, Trabajo Final de Licenciatura, 143 pp., Departamento de Geología, Facultad de Ciencias Exactas y Naturales, Universidad de Buenos Aires, trabajo inédito.

Brooks, B. A., M. Bevis, R. Smalley Jr., E. Kendrick, R. Manceda, E. Lauría, R. Maturana, and M. Araujo (2003), Crustal motion in the Southern Andes (26° 36°S): Do the Andes behave like a microplate?, *Geochem. Geophys. Geosyst.*, *4*(10), 1085, doi:10.1029/2003GC000505.

Cahill, T., and B. L. Isacks (1992), Seismicity and shape of the subducted Nazca plate, *J. Geophys. Res.*, *97*, 17,503–17,529.

Casa, A. L. (2005), Geología y neotectónica del piedemonte oriental del cordón del Plata en los alrededores de El Salto, provincia de Mendoza, Trabajo Final de Licenciatura, 174 pp., Departamento de Geología, Facultad de Ciencias Exactas y Naturales, Universidad de Buenos Aires, trabajo inédito.

Coblentz, D. D., and R. M. Richardson (1996), Analysis of the South American intraplate stress field, *J. Geophys. Res.*, *101*, 8643–8657.

Colmenares, L., and M. D. Zoback (2003), Stress field and seismotectonics of northern South America, *Geology*, *31*(8), 721–724.

Cortés, J. M., P. Vinciguerra, M. Yamín, and M. M. Pasini (1999), Tectónica Cuaternaria de la Región Andina del Nuevo Cuyo (28°–38° LS), in *Geología Argentina. Subsecretaría de Minería de la Nación*, edited by R. Caminos, *Serv. Geol. Min. Argent. An.*, *29*(24), 760–778.

Cortés, J. M., L. Fauqué, M. Yamín, A. Folguera, M. Etcheverría, and M. Pisan (2000), Geometric patterns of Quaternary structure in western Precordillera and cordon del Plata (30°30′–33°30′SL), in *Flat-Slab Subduction in Present and Ancient Orogens, IGCP 453 "Modern and Ancient Orogens", Transcuyo Working Group – ICL C.C.4. Joint Meeting (Mendoza)*, Program with Abstracts, pp. 8–9.

Cortés, J. M., A. Casa, M. M. Pasini, and M. Yamín (2005), Fajas de estructuras neotectónicas asociadas a rasgos paleotectónicos en Precordillera sur y Cordillera (31°30′–33°30′ LS), paper presented at XVI Congreso Geológico Argentino, Asoc. Geol. Arg., La Plata, Argentina.

Dalmayarc, B., and P. Molnar (1981), Parallel thrust and normal faulting in Peru and constraints on the state of stress, *Earth Planet. Sci. Lett.*, *55*, 473–481.

García, V. (2004), Análisis estructural y geotectónico de las Lomas Jaboncillo y del Peral, departamento de Tupungato, provincia de Mendoza, Trabajo Final de Licenciatura, 100 pp., Departamento de Geología, Facultad de Ciencias Exactas y Naturales, Universidad de Buenos Aires, trabajo inédito.

García, V., E. Cristallini, J. Cortés, and M. C. Rodriguez (2004), Estructura y Neotectónica de los anticlinales Jaboncillo y del Peral, Departamento de Tupungato, provincia de Mendoza, paper presented at XXII Reunión de Microtectónica y Geología Estructural, Cafayate, Salta.

Gutscher, M. A., W. Spakman, H. Bijwaard, and E. R. Engdahl (2000), Geodynamics of flat subduction: Seismicity and tomographic constraints from the Andean margin, *Tectonics*, *19*, 814–833.

Guzmán, C. (2007), Estudio de la deformación andina entre los 32° y los 39° latitud sur mediante el análisis de breakout de pozos, Tesis doctoral, 241 pp., Departamento de Geología, Facultad de Ciencias Exactas y Naturales, Universidad de Buenos Aires, trabajo inédito.

Guzmán, C., E. Cristallini, and G. Bottesi (2007), Contemporary stress orientations in the Andean retroarc between 34°S and 39°S from borehole breakout analysis, *Tectonics*, *26*, TC3016, doi:10.1029/2006TC001958.

INPRES (1982), Microzonación Sísmica del Valle de Tulum-Provincia de San Juan, *Inf. Téc. Gen.*, vol. 1–3.

INPRES (1995), Microzonificación Sísmica del Gran Mendoza, *Resumen Ejecutivo*, 283 pp., Publicación Técnica.

Isacks, B. L., T. E. Jordan, R. W. Allmendinger, and V. A. Ramos (1982), La segmentación tectónica de los Andes Centrales y su relación con la geometría de la placa de Nazca subductada, paper presented at V° Congreso Latinoamericano de Geología, Argentina.

Jordan, T., B. Isacks, R. Allmendigner, J. Brewer, V. Ramos, and C. Ando (1983), Andean tectonics related to geometry of the subducted Nazca plate, *Geol. Soc. Am. Bull.*, *94*, 341–361.

Kadinsky-Cade, K., R. Reilinger, and B. Isacks (1985), Surface deformations associated with the November 23, 1977, Caucete, Argentina, earthquake sequence, *J. Geophys. Res.*, *90*, 12,691–12,700.

Kay, S. M., and J. M. Abbruzzi (1996), Magmatic evidence for Neogene lithospheric evolution of the Central Andean "flat-slab" between 30° and 32°S, *Tectonophysics*, *259*, 15–28.

Kendrick, E., M. Becis, R. Smalley Jr., B. Brooks, R. B. Vargas, E. Lauría, and L. P. Souto Fortes (2003), The Nazca-South America Euler vector and its rate of change, *J. South Am. Earth Sci.*, *16*, 125–131.

Kendrick, E., B. A. Brooks, M. Bevis, R. Smalley Jr., E. Lauria, M. Araujo, and H. Parra (2006), Avtive orogeny of the South-Central Andes studied with GPS geodesy, *Rev. Asoc. Geol. Argent.*, *61*(4), 555–566.

Kozlowski, E. E., R. Manceda, and V. Ramos (1993), Estructura, in *Geología y Recursos Naturales de Mendoza*, edited by V. Ramos, *Relatorio I*(18), pp. 235–256, Asoc. Geol. Arg., Buenos Aires, Argentina.

Legarreta, L., D. A. Kokogian, and D. A. Dellapé (1992), Estructuración terciaria de la Cuenca Cuyana: ¿Cuánto de inversión tectónica?, *Rev. Asoc. Geol. Argent.*, *47*(1), 83–86.

Lima, C., E. Nascimiento, and M. Assumpçao (1997), Stress orientations in Brazilian sedimentary basins from breakout análisis: Implications for force models in the South American plate, *Geophys. J. Int.*, *130*, 112–124.

Mardia, K. V. (1972), *Statistics of Directional Data: Probability and Mathematical Statistics*, 357 pp., Elsevier, New York.

Meijer, P. T., R. Govers, and M. J. R. Wortel (1997), Forces controlling the present-day state of stress in the Andes, *Earth Planet. Sci. Lett.*, *148*, 157–170.

Miranda, S., and J. A. Robles (2002), Posibilidades de atenuación cortical en la cuenca Cuyana a partir del análisis de datos de gravedad, *Rev. Asoc. Geol. Argent.*, *57*(3), 271–279.

Mpodozis, C., and V. A. Ramos (1989), The Andes of Chile and Argentina, in *Geology of the Andes and Its Relation to Hydrocarbon and Mineral Resources*, *Circum-Pacific Council for Energy and Mineral Resources*, edited by G. E. Ericksen, M. T. Cañas Pinochet, and J. A. Reinemund, *Earth Sci. Ser.*, *11*, 59–90.

National Earthquake Information Center (NEIC) (2008), USGS, global seismic database on earthquake. (Available at http://neic.usgs.gov/neis/epic/epic_rect.html)

Norabuena, E., T. Dixon, S. Stein, and C. G. A. Harrison (1999), Decelerating Nazca-South America and Nazca-Pacific motions, *Geophys. Res. Lett.*, *26*, 3405–3408.

Pilger, R. H. (1981), Plate reconstructions, aseismic ridges, and low angle subduction beneath the Andes, *Geol. Soc. Am. Bull.*, *92*, 448–456.

Ramos, V. A. (1985), The tectonics of the Central Andes (30°–33°S), paper presented at Symposium on Processes in Continental Lithospheric Deformation, Abstracts, Yale Univ., New Haven.

Ramos, V. A. (1988), The tectonics of the Central Andes: 30° to 33°S latitude, in *Processes in Continental Lithospheric Deformation*, edited by S. Clark and D. Burchfiel, *Geol. Soc. Am. Spec. Pap.*, *218*, 31–54.

Ramos, V. A., M. Cegarra, and E. O. Cristallini (1996), Cenozoic tectonics of the high Andes of west-central Argentina (30°–36°S latitude), *Tectonophysics*, *259*, 185–200.

Reinecker, J., M. Tingay, and B. Müller (2004), Borehole breakout analysis from four-arm caliper logs. (Available at www.world-stress-map.org)

Reinecker, J., O. Heidbach, M. Tingay, B. Sperner, and B. Müller (2005), The 2005 release of the World Stress Map. (Available at www.world-stress-map.org)

Richardson, R. M., and D. D. Coblentz (1994), Stress modelling in the Andes: Constraints on South American intraplate stress magnitudes, *J. Geophys. Res.*, *99*, 22,015–22,025.

Sarewitz, D. (1988), High rate of Late Cenozoic crustal shortening in the Andean foreland, Mendoza province, Argentina, *Geology*, *16*(12), 1138–1142.

Siame, L. L., O. Bellier, M. Sebrier, and M. Araujo (2005), Deformation partitioning in flat subduction setting: Case of the Andean foreland of western Argentina (28°S–33°S), *Tectonics*, *24*, TC5003, doi:10.1029/2005TC001787.

Siame, L. L., O. Bellier, and M. Sebrier (2006), Active tectonics in the Argentine Precordillera and western Sierras Pampeanas, *Rev. Asoc. Geol. Argent*, *61*(4), 604–619.

Smalley, R., Jr., and B. L. Isacks (1990), Seismotectonics of thin- and thick-skinned deformation in the Andean foreland from local network data: Evidence for a seismogenic lower crust, *J. Geophys. Res.*, *95*, 12,487–12,498.

Sperner, B., B. Müller, O. Heidbach, D. Delvaux, J. Reinecker, and K. Fuchs (2003), Tectonic stress in the earth's crust: Advances in the World Stress Map Project, in *New Insights into Structural Interpretation and Modeling*, edited by D. Nieuwland, *Geol. Soc. London Spec. Publ.*, *212*, 101–116.

Tingay, M., B. Müller, J. Reinecker, O. Haidbach, F. Wenzel, and P. Fleckenstein (2005), The World Stress Map Project "Present-day stress in sedimentary basins" initiative: Building a valuable public resource to understand tectonic stress in the oil patch, *Lead. Edge*, *24*(12), 1276–1282.

Uliana, M. A., and K. T. Biddle (1988), Mesozoic–Cenozoic paleogeographic and geodynamic evolution of southern South America, *Rev. Bras. Geocienc.*, *18*, 172–190.

Uliana, M. A., M. E. Arteaga, L. Legarreta, J. J. Cerdán, and G. Peroni (1995), Inversion structures and hydrocarbon occurrence in Argentina, in *Basin Inversion*, edited by J. G. Buchman and P. G. Buchman, *Geol. Soc. London Spec. Publ.*, *88*, 211–233.

Vergés, J., V. A. Ramos, A. Meigs, E. Cristallini, F. H. Bettini, and J. M. Cortés (2007), Crustal wedging triggering recent deformation in the Andean thrust front between 31°S and 33°S: Sierras Pampeanas-Precordillera interaction, *J. Geophys. Res.*, *112*, B03S15, doi:10.1029/2006JB004287.

Zerwer, A., and N. A. Yassir (1994), Borehole breakout interpretation in the Gulf Coast, offshore Louisiana, in *Rock Mechanics*, edited by Nelson and Laubach, pp. 225–232, A. A. Balkema, Brookfield, Vt.

Zoback, M. L. (1992), The first and second order patterns of stress in the lithosphere: The World Stress Map Project, *J. Geophys. Res.*, *97*, 11,703–11,728.

Zoback, M. L., and M. D. Zoback (1989), Tectonic stress field of the conterminous United States, in *Geophysical Framework of the Continental United States*, edited by L. C. Pakiser and W. D. Mooney, *Mem. Geol. Soc. Am.*, *172*, 523–539.

Zoback, M. D., and M. L. Zoback (1991), Tectonic stress field of North America and relative plate motions, in *Neotectonics of North America Decade Map Volume I*, edited by D. B. Slemmons et al., pp. 339–366, Geol. Soc. of Am., Boulder, Colo.

E. O. Cristallini and C. G. Guzmán, Laboratorio de Modelado Geológico, Departamento de Ciencias Geológicas, Universidad de Buenos Aires, Pabellón II, Ciudad Universitaria, Buenos Aires C1428EHA, Argentina. (ceciliagguzman@hotmail.com)

American Geophysical Union
Author Query Form

Journal: **Journal of Geophysical Research - Solid Earth**
Article Name: **Guzmán(2007JB005505)**

Please answer all author queries.

1. Please provide volume number and page range of "Alvarado et al. (2005)" in the reference list.

2. Please provide publisher name of "Cortés et al. (1999)" in the reference list.

3. Please provide publisher name and location of "Cortés et al. (2000)" in the reference list.

4. Please provide date of meeting of the following references:

   - Cortés et al. (2005)
   - García et al. (2004)

5. Please provide the page range of "INPRES, 1982" in the reference list.

6. Please provide publisher location of "INPRES, 1995" in the reference list.

7. Please provide the date of the symposium of "Ramos, 1985" in the reference list.

8. Please provide university location of the following references:

   - Borgnia (2004)
   - Casa (2005)
   - García (2004)
   - Guzmán (2007)

9. Please provide sponsor name and date of meeting of the following references:

   - Isacks et al. (1982)
   - Ramos (1985)

10. Please provide page information and publisher name of the following references:

    - National Earthquake Information Center (NEIC) (2008)
    - Reinecker et al. (2004)
    - Reinecker et al. (2005)